[Chem. Pharm. Bull. 33(12)5464—5473(1985)]

Influence of Wetting Factors on the Dissolution Behavior of Flufenamic Acid[1)]

SHIGERU ITAI,*[,a] MASAMI NEMOTO,[a] SHOZO KOUCHIWA,[a] HIROSHI MURAYAMA[a] and TSUNEJI NAGAI[b]

Research Laboratory, Taisho Pharmaceutical Co., Ltd.,[a] Yoshino-cho 1-403, Omiya, Saitama 330, Japan and Faculty of Pharmaceutical Science, Hoshi University,[b] Evara 2-4-41, Shinagawa-ku, Tokyo 142, Japan

(Received April 4, 1985)

The effects of surfactant, particle size, and additives on the dissolution rate of flufenamic acid (FFA) were evaluated in relation to the time course of the available surface area ($S(t)$).

The ratios of $S(t)$ generated by time t to the total $S(t)$ generated during the dissolution process ($F(t)$), obtained from the dissolution rate study, were well regressed to the Weibull probability distribution functions. By using the probability parameters obtained, it was possible to elucidate the influence of these factors on the surface characteristics of FFA quantitatively. When the concentration of the surfactant employed was below the critical micelle concentration (cmc), the initial $S(t)$ generated was significantly increased as the surfactant concentration of the dissolution medium increased. Above the cmc, however, the increase was not so marked. The micronization of particles has a significant enhancing effect on the $S(t)$ generated when the surfactant concentration in the dissolution medium was at cmc. The influence of numerous additives on the dissolution rate of FFA and the $S(t)$ generated is also described.

Keywords——dissolution profile; available surface area; linear regression; surface characteristic; critical micelle concentration (cmc); particle size; flufenamic acid

Many factors influence the dissolution behavior of solid dosage forms, but from a pharmacotechnological viewpoint, one of the most important of these is the surface characteristics of the active ingredient in the preparation. A reduction of particle size through micronization is commonly employed to improve the dissolution rate of a water-insoluble drug. However, excessive micronization results in a considerable increase in the hydrophobicity of the active ingredient and a decrease of the available surface area. Finholt *et al.*[2)] reported that the dissolution rates of phenobarbital, aspirin and phenacetin are decreased by the reduction of their particle sizes. On the other hand, the influence of surfactants on drug dissolution has been investigated extensively. However, few reports[3,4)] have dealt with the dissolution behavior of powdered drugs having controlled particle sizes, in surfactant solution.

In our previous study,[5)] time course equations were derived for $S(t)$ generated in the dissolution process, and the influence of the manufacturing process on the dissolution of flufenamic acid (FFA) in tablets was evaluated. In the present study, the dissolution rate of FFA powders in various concentrations of polysorbate 80 was determined. Then, by using the previous method, the available surface area of FFA powders was obtained quantitatively.

Experimental

Materials——FFA and polyvinylpyrrolidone (PVP) were of commercial grade. Corn starch (CS), carboxymethylcellulose calcium (CMC-Ca), microcrystalline cellulose (MCC) and magnesium stearate (St. Mg) were all of

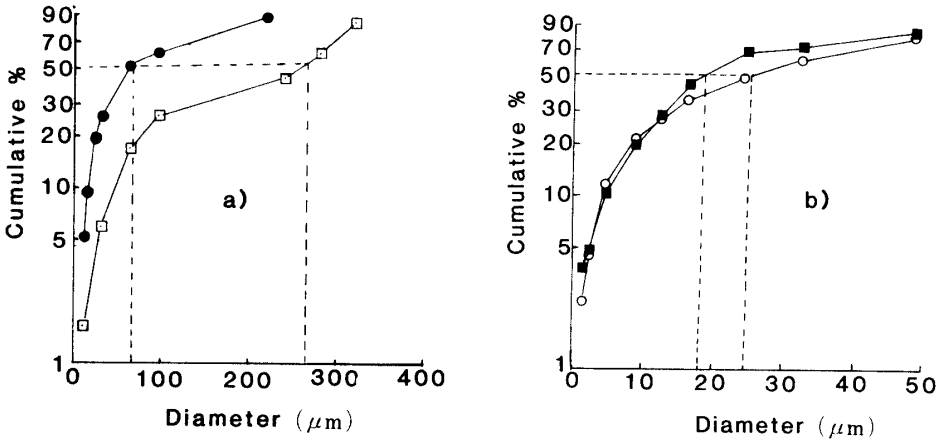

Fig. 1. Particle Size Distributions of FFA Powders
⊡, 42—48 mesh; ●, 60—65 mesh; ○, powders passed through 150 mesh; ■, micronized powders obtained by crystallization.

JP X grade. All other chemicals were of reagent grade. Some of the FFA samples were sieved through Japan Industrial Standard (JIS) sieves and 42—48 and 60—65 mesh particle fractions and particles that passed through 150 mesh were collected for use in this study. The remaining fine material was crystallized from 1 N sodium hydroxide solution by adding an equal amount of 1 N hydrochloric acid. The arithmetic mean diameter of 42—48 and 60—65 mesh particles was taken as the mean size of the particle size distributions, measured using a laser granulometer, model 715 (Compagnie Industrielle des Lasers), for particles smaller than 192 μm and a microscope for particles larger than 192 μm. The particle size distributions of the powders that passed through 150 mesh and the micronized powders obtained by crystallization were measured using a laser granulometer (model 715). The results are shown in Fig. 1; the mean diameters of 42—48 and 60—65 mesh particles, particles that passed through 150 mesh and the micronized particles obtained by crystallization were determined to be 263, 76.0, 24.2 and 17.7 μm, respectively.

Preparations of FFA–Additive Mixtures——FFA (5 g) was dissolved in 50 ml of acetone. The same amount of an additive was added to the solution, which was then rapidly shaken for 30 s. After evaporation of the acetone, the powdered mixture was passed through a 60 mesh sieve.

Determination of the Dissolution Rate Constant per Unit Surface Area——The rotating disk method was applied to determine the dissolution rate constant per unit surface area (k) of FFA in pH 6.24 phosphate buffer solutions containing from 0 to 1% (w/v) polysorbate 80. The method was identical with the procedure used in our previous study.[5]

Solubility Determination——The solubility of FFA was determined in a series of pH 6.24 phosphate buffer solutions containing various concentrations of polysorbate 80. FFA in excess of the amount required for saturation solubility was added to 30 ml of the surfactant solution contained in a 50-ml centrifuge tube and the tube was then shaken in a water bath at 37 °C for 24 h. Results were obtained spectrophotometrically using the same method as in our previous study.[5]

Dissolution Study——Dissolution of FFA powders of various particle sizes and the FFA–additive mixtures was tested in a USP dissolution test apparatus using Method II: FFA powder (100 mg) or FFA–additive mixture (200 mg) in pH 6.24 phosphate buffer solutions containing various concentrations of polysorbate 80 was agitated at 100 rpm and 37 °C. Aliquots (1 ml) of each sample solution were withdrawn at appropriate time intervals through a membrane filter (pore size: 0.45 μm) and immediately diluted with 99 ml of the phosphate buffer. The absorbance was determined at 288 nm with a spectrophotometer and the FFA concentration was calculated from the absorbance of the standard solution. The dissolution test was performed at least twice, and showed high reproducibility.

Measurement of the Surface Tension of Polysorbate 80 Solutions——The surface tension of pH 6.24 phosphate buffer solutions containing various concentrations of polysorbate 80 was measured with a tensiometer (Kodaira Seisakushyo) at 37 °C using a 2-cm platinum–iridium ring.

Measurement of Viscosity of Polysorbate 80 Solutions——The viscosity of the solutions was measured at 37 °C using a viscometer. The densities of the solutions were measured using a pycnometer.

Results and Discussion

Determination of the Specific Surface Area of the Powders

If the particles are spherical, the specific surface area (S_w) of the powders can be obtained

from Eq. 1:

$$S_w = \sum 6P/(\rho \cdot \mu) \quad (1)$$

where P is the ratio of the weight of particles in a fraction to the total weight of the distributed powders, ρ is the density of FFA ($=1.49\,g/cm^3$) and μ is the mean diameter of the particles in a fraction. From Eq. 1, the values of initial surface area ($S(0)$) of the powders were determined to be 45.3, 120.6, 3.84×10^2 and $4.27 \times 10^2\,cm^2$ per 100 mg for 42—48 and 60—65 mesh particle fractions, particles that passed through 150 mesh and micronized powders obtained by crystallization, respectively.

Physicochemical Properties of Phosphate Buffer Solutions Containing Various Concentrations of Polysorbate 80

The results of measurements of surface tension, density and viscosity of the surfactant solutions are shown in Table I. Below 1% (w/v) surfactant concentration (selected in this study), the density and the viscosity of the solution scarcely varied. On the other hand, the surface tension decreased as the concentration of the surfactant in the solution increased. However, above 10^{-2}% (w/v) surfactant concentration, the amount by which the surface tension was lowered by increasing the concentration of the surfactant was not large.

Determination of *k*

The results of dissolution of a 2-cm FFA disk using the rotating disk method are shown in Fig. 2. An approximately linear relationship existed between time and the amount of FFA dissolved. If $C_s \gg C$ (sink condition) and the available surface area is constant, then by rearrangement and integration of the Noyes–Whitney equation:[6]

$$C = k \cdot S \cdot C_s / V \cdot t \quad (2)$$

where C_s is the solubility, S is the available surface area, V is the solvent volume and C is the solute concentration. From the slopes of the curves in Fig. 2, the dissolution rate constants per unit surface area (k) could be obtained. The values of k as well as C_s of FFA in the surfactant solutions are shown in Table II and the data for k, C_s and surface tension are plotted *vs.* the surfactant concentration in Fig. 3. As shown in Fig. 3, the curves for C_s and k as well as surface tension showed an inflection at 10^{-2}% (w/v). That is to say, when concentrations below 10^{-2}% (w/v) were employed, the values of C_s and k were constant and independent of the concentration of polysorbate 80, whereas when concentrations above 10^{-2}% (w/v) were used, the values of C_s and k linearly increased and decreased, respectively, as the concentration of polysorbate 80 increased. These results indicate that the cmc of polysorbate 80 is

TABLE I. Physicochemical Properties of pH 6.24 Phosphate Buffer Solutions Containing Various Concentrations of Polysorbate 80

Surfactant concn. (% (w/v))	Surface tension (dyn/cm)	Density (g/cm^3)	Viscosity (cP)
0	74.6	1.136	0.884
10^{-4}	65.4	1.136	0.887
10^{-3}	50.1	1.136	0.921
10^{-2}	42.4	1.136	0.896
5×10^{-2}	—	1.137	0.887
10^{-1}	43.4	1.137	0.896
2×10^{-1}	—	1.138	0.907
1	40.1	—	—

—: not measured.

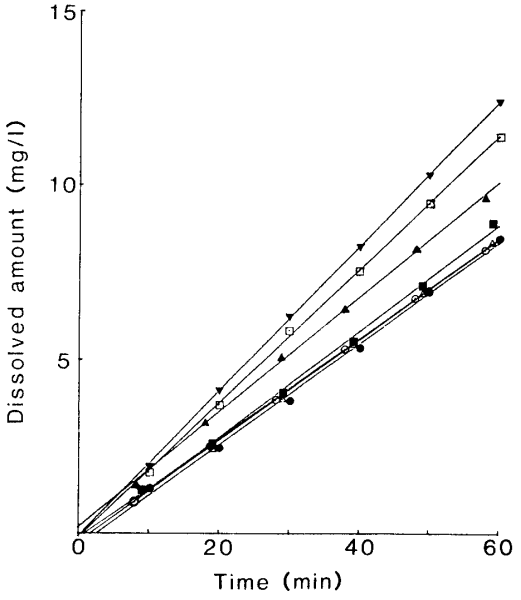

Fig. 2. Dissolution Rate of an FFA Disk using the Rotating Disk Method in pH 6.24 Phosphate Buffer Solutions Containing Various Concentrations of Polysorbate 80 ($S=3.14$ cm^2; $V=900$ ml)

⊙, 0% (w/v); △, 10^{-4}% (w/v); ●, 10^{-3}% (w/v); ■, 10^{-2}% (w/v); ▲, 5×10^{-2}% (w/v); □, 10^{-1}% (w/v); ▼, 2×10^{-1}% (w/v).

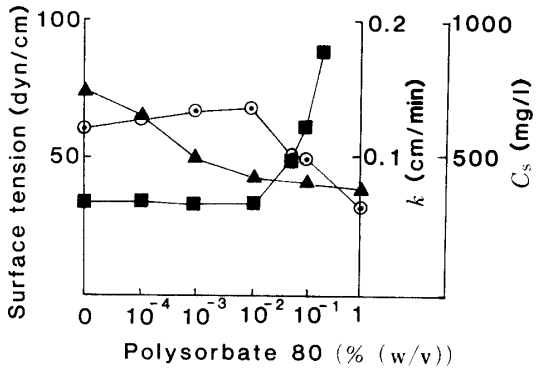

Fig. 3. C_s, k and Surface Tension *versus* Polysorbate 80 Concentration in pH 6.24 Phosphate Buffer Solution

■, C_s; ⊙, k; ▲, surface tension.

TABLE II. Dissolution Rate Constant per Unit Surface Area (k) of FFA in pH 6.24 Phosphate Buffer Solutions Containing Various Concentrations of Polysorbate 80

Surfactant concn. (% (w/v))	Rotating disk method			C_s (mg/l)	k (cm/min)
	Slope	y-Intercept	r [a]		
0	0.145	0.230	0.9999	337.4	0.123
10^{-4}	0.144	0.172	0.999	343.2	0.120
10^{-3}	0.146	0.379	0.998	334.1	0.125
10^{-2}	0.153	0.322	0.998	341.6	0.128
5×10^{-2}	0.165	0.177	0.999	493.2	0.096
10^{-1}	0.192	0.120	0.999	619.3	0.089
2×10^{-1}	0.208	0.089	0.9999	888.8	0.067

a) Correlation coefficient.

about 10^{-2}% (w/v), and the increase of C_s above the cmc is considered to be due to micelle solubilization. On the other hand, since the viscosity of the surfactant solutions employed in this study was almost constant, the decrease of k above the cmc is considered to be due to the lowering of the diffusion rate by micelle formation.

Effect of Polysorbate 80 Concentration on the Available Surface Area of FFA

In our previous study,[5] we derived time course equations for $S(t)$ generated in the dissolution process and also for the dissolution rate in relation to $S(t)$, as shown in Eqs. 3 and 4:

$$S(t)=V/k\cdot\ln\{C_s/(C_s-W_0/V)\}\cdot dF(t)/dt \quad (3)$$

$$C = C_s[1 - \exp[-[\ln\{C_s/(C_s - W_0/V)\} \cdot F(t)]]] \quad (4)$$

where $F(t)$ is interpreted as the ratio of the cumulative surface area which has been made available for dissolution up to time t to the total surface area which is made available during the dissolution process.[7] This can be calculated from the experimental data by using Eq. 5:

$$F(t) = \ln\{C_s/(C_s - C)\}/\ln\{C_s/(C_s - W_0/V)\} \quad (5)$$

Furthermore, $F(t)$ can be interpreted as a cumulative probability distribution, and if the Weibull distribution is selected,

$$F(t) = 1 - \exp\{-(t^b/a)\} \quad (6)$$

Eq. 6 may be rearranged into

$$\ln \cdot \ln\{1/(1 - F(t))\} = b \cdot \ln t - \ln a \quad (7)$$

The $\ln \cdot \ln - \ln$ plot (Weibull plot) of $1/(1 - F(t))$ *vs.* t therefore becomes linear and parameters a and b can be obtained from the y-intercept and the slope of the line. Weibull plots for $F(t)$ of FFA that passed through 150 mesh in pH 6.24 phosphate buffer solutions containing polysorbate 80 are shown in Fig. 4. Each set of $F(t)$ data for FFA in the surfactant solutions showed a linear relation. The values of the probability parameters are shown in Table III. By taking T_{20}, T_{50} and T_d as the times when 20%, 50% and 63.2%, respectively, of the available surface area has been generated during the dissolution process, the following expressions can be obtained:

$$T_{20} = \sqrt[b]{a \cdot \ln 1.25} \quad (8)$$

$$T_{50} = \sqrt[b]{a \cdot \ln 2} \quad (9)$$

$$T_d = \sqrt[b]{a} \quad (10)$$

By substituting the determined values (a, b) of the Weibull distribution into Eqs. 3 and 4, the

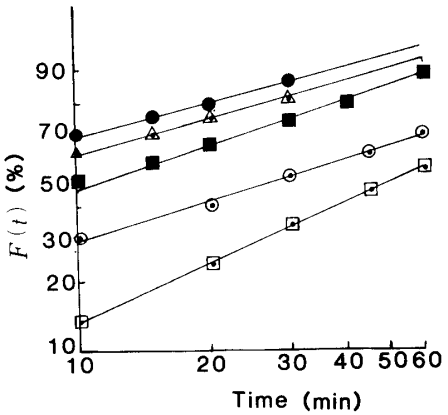

Fig. 4. Weibull Plots for $F(t)$ of FFA Powders that Passed through 150 mesh in pH 6.24 Phosphate Buffer Solutions Containing Various Concentrations of Polysorbate 80

⊡, 0% (w/v); ⊙, 10^{-2}% (w/v); ■, 5×10^{-2}% (w/v); △, 10^{-1}% (w/v); ●, 2×10^{-1}% (w/v).
The regression lines were determined with the $F(t)$ data from 10 to 90%, since the Weibull plot is sensitive in this range.

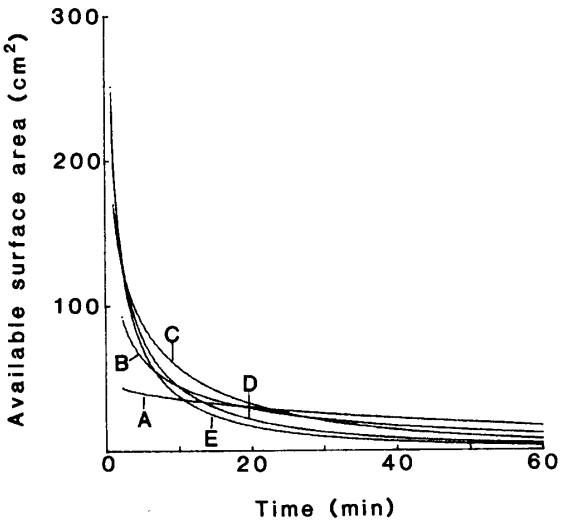

Fig. 5. $S(t)$ *vs.* t Patterns of FFA Powders that Passed through 150 mesh in pH 6.24 Phosphate Buffer Solutions Containing Various Concentrations of Polysorbate 80

A, 0% (w/v); B, 10^{-2}% (w/v); C, 5×10^{-2}% (w/v); D, 10^{-1}% (w/v); E, 2×10^{-1}% (w/v).

TABLE III. Probability Parameters of the Weibull Distribution in Fig. 4

Surfactant concn. (% (w/v))	a	b	T_{20} (min)	T_{50} (min)	T_d (min)
0	58.0	0.935	15.5	52.0	76.9
10^{-2}	12.9	0.651	5.1	28.9	50.8
5×10^{-2}	8.60	0.721	2.5	11.9	19.8
10^{-1}	4.50	0.603	1.0	6.6	12.1
2×10^{-1}	3.43	0.569	0.6	4.6	8.7

TABLE IV. Available Surface Area of FFA Powders That Passed through 150 Mesh in pH 6.24 Phosphate Buffer Solutions Containing Various Concentrations of Polysorbate 80

Surfactant concn. (% (w/v))	Available surface area (cm^2/100 mg FFA) Time (min)									
	2	4	6	8	10	15	20	30	45	60
0	43.6	40.4	38.2	36.5	35.0	31.8	29.2	25.0	20.1	16.3
10^{-2}	97.0	71.1	58.2	50.0	44.2	34.5	28.5	21.0	14.7	11.0
5×10^{-2}	136.5	99.4	79.7	66.7	57.2	41.5	31.7	20.1	11.4	6.9
10^{-1}	145.2	92.5	68.4	53.9	44.1	29.3	21.1	12.3	6.5	3.8
2×10^{-1}	143.2	86.2	61.3	46.9	37.4	23.7	16.5	9.1	4.5	2.5

TABLE V. Dissolution Rate of FFA Powders That Passed through 150 Mesh in pH 6.24 Phosphate Buffer Solutions Containing Various Concentrations of Polysorbate 80

Surfactant concn. (% (w/v))	Dissolved amount (mg/900 ml) Time (min)						
	5	10	15	20	30	45	60
0	—	16.4[a]	—	27.8	39.1	50.8	59.2
	(8.9)[b]	(16.3)	(22.8)	(28.5)	(38.6)	(50.4)	(59.6)
10^{-2}	—	34.2	—	45.4	56.0	64.9	72.1
	(23.1)	(33.5)	(41.0)	(46.8)	(55.7)	(64.9)	(71.4)
5×10^{-2}	32.9	50.3	59.5	66.6	75.5	—	81.5
	(33.8)	(48.9)	(59.1)	(66.4)	(76.5)	(85.3)	(90.4)
10^{-1}	46.4	61.4	70.5	76.6	82.9	—	87.5
	(46.8)	(61.3)	(70.1)	(76.0)	(83.6)	(89.9)	(93.4)
2×10^{-1}	52.7	68.3	76.1	80.4	87.3	—	94.2
	(53.4)	(67.5)	(75.6)	(80.9)	(87.5)	(92.6)	(95.3)

—: not measured. *a*) Experimental data. *b*) Regression data of Weibull distribution.

time course of $S(t)$ and the dissolution rate of the FFA powders in relation to $S(t)$ could be obtained. The $S(t)$ values of FFA in the surfactant solutions and the patterns obtained are shown in Table IV and Fig. 5. The initial values of $S(t)$ and its rate of decrease due to dissolution increased as the concentration of polysorbate 80 in the solvent was increased. However, above the cmc (10^{-2}% (w/v)) of the surfactant, this enhancement was not so marked.

The results of the dissolution test as well as the regression curves calculated from Eq. 4 are shown in Table V and Fig. 6, respectively. Since the experimental data coincided with the

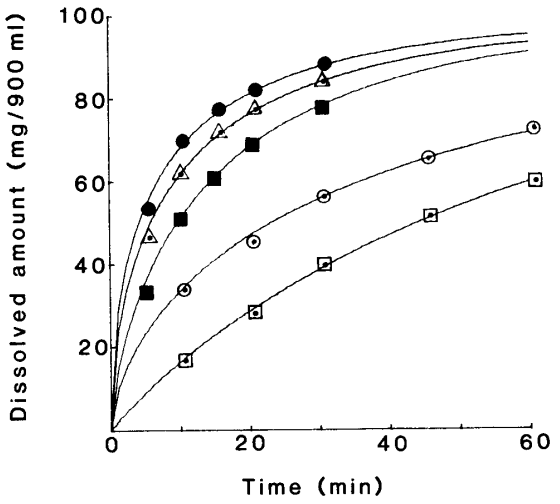

Fig. 6. Dissolution Profiles of FFA Powders that Passed through 150 mesh in pH 6.24 Phosphate Buffer Solutions Containing Various Concentrations of Polysorbate 80 ($W_0 = 100$ mg; $V = 900$ ml)

The full lines are the regression curves of the Weibull distribution.
⊡, 0% (w/v); ⊙, 10^{-2}% (w/v); ■, 5×10^{-2}% (w/v); △, 10^{-1}% (w/v); ●, 2×10^{-1}% (w/v).

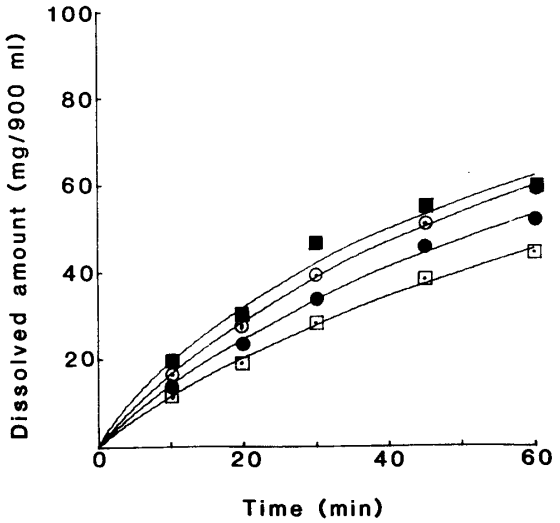

Fig. 7. Dissolution Profiles of FFA Powders with Various Particle Sizes in pH 6.24 Phosphate Buffer Solution ($W_0 = 100$ mg; $V = 900$ ml)

The full lines are the regression curves of the Weibull distribution.
⊡, 42—48 mesh; ●, 60—65 mesh; ⊙, 150 mesh pass; ■, micronized powders obtained by crystallization.

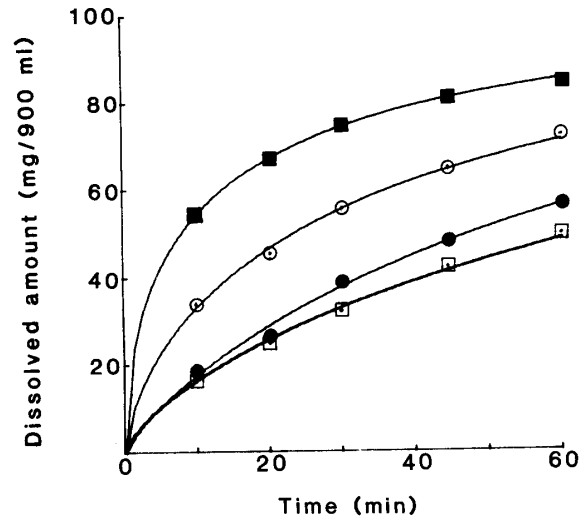

Fig. 8. Dissolution Profiles of FFA Powders with Various Particle Sizes in pH 6.24 Phosphate Buffer Solution Containing Polysorbate 80 at the cmc ($W_0 = 100$ mg; $V = 900$ ml)

The full lines are the regression curves of the Weibull distribution.
The symbols are the same as in Fig. 7.

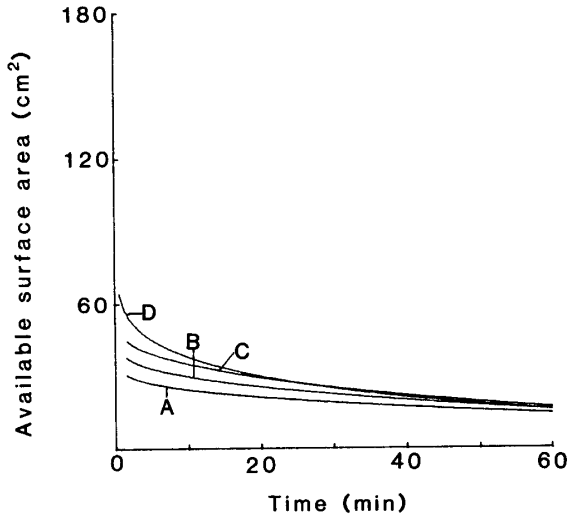

Fig. 9. $S(t)$ *vs.* t Patterns of FFA Powders with Various Particle Sizes in pH 6.24 Phosphate Buffer Solution

A, 42—48 mesh; B, 60—65 mesh; C, 150 mesh pass; D, micronized powders obtained by crystallization.

regression curves, the $S(t)$ values in Table IV and the patterns in Fig. 5 were assumed to be reasonable.

Effect of Particle Size on the Available Surface Area of FFA

The results of the dissolution test using 42—48, 60—65 and 150 mesh powder fractions and micronized powders obtained by crystallization, in the phosphate buffer solution and the

TABLE VI. Probability Parameters of the Weibull Distribution in Figs. 7 and 8

Samples	a	b	T_{20} (min)	T_{50} (min)	T_d (min)
42—48 mesh	82.3[a]	0.915	24.1	83.1	124.0
	(37.2)[b]	(0.748)	(16.9)	(77.1)	(125.8)
60—65 mesh	68.2	0.928	18.8	63.8	94.6
	(41.2)	(0.830)	(14.5)	(56.7)	(88.2)
150 mesh pass	58.0	0.935	15.5	52.0	76.9
	(12.9)	(0.651)	(5.1)	(28.9)	(50.8)
Micronized powders	41.5	0.869	13.0	47.7	72.8
	(4.88)	(0.526)	(1.2)	(10.1)	(20.4)

a) Data in pH 6.24 phosphate buffer solution. *b*) Data in pH 6.24 phosphate buffer solution containing 10^{-2}% (w/v) polysorbate 80.

TABLE VII. Available Surface Area of FFA Powders with Various Particle Sizes

Samples	Available surface area (cm^2/100 mg FFA) Time (min)									
	2	4	6	8	10	15	20	30	45	60
42—48 mesh	29.9[a]	27.7	26.2	25.1	24.2	22.3	20.9	18.5	15.8	13.7
	(44.6)[b]	(36.4)	(32.0)	(29.0)	(26.8)	(22.9)	(20.3)	(16.8)	(13.4)	(11.2)
60—65 mesh	36.8	34.1	32.4	31.0	29.8	27.3	25.3	22.1	18.3	15.4
	(47.4)	(40.8)	(36.9)	(34.1)	(32.0)	(27.9)	(25.0)	(20.8)	(16.5)	(13.4)
150 mesh pass	43.6	40.4	38.2	36.5	35.0	31.8	29.2	25.0	20.1	16.3
	(97.0)	(71.1)	(58.2)	(50.0)	(44.2)	(34.5)	(28.5)	(21.0)	(14.7)	(11.0)
Micronized powders	53.5	47.1	43.1	40.2	37.9	33.3	29.9	24.7	19.2	15.4
	(159.8)	(101.1)	(75.4)	(60.4)	(50.3)	(35.3)	(26.8)	(17.5)	(10.8)	(7.3)

a) Data in pH 6.24 phosphate buffer solution. *b*) Data in pH 6.24 phosphate buffer solution containing 10^{-2}% (w/v) polysorbate 80.

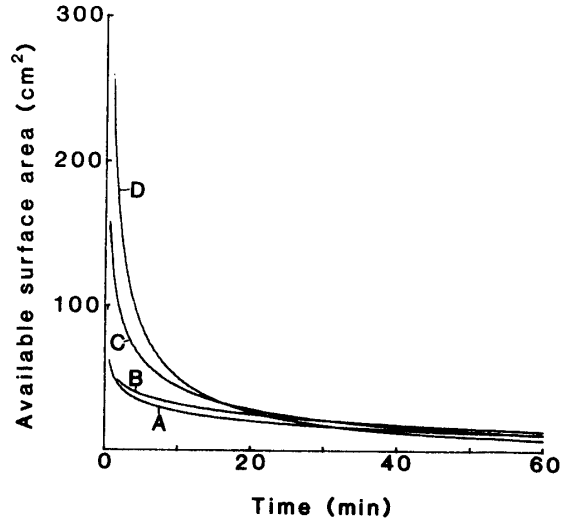

Fig. 10. $S(t)$ *vs.* t Patterns of FFA powders with Various Particle Sizes in pH 6.24 Phosphate Buffer Solution Containing Polysorbate 80 at the cmc

A, 42—48 mesh; B, 60—65 mesh; C, 150 mesh pass; D, micronized powders obtained by crystallization.

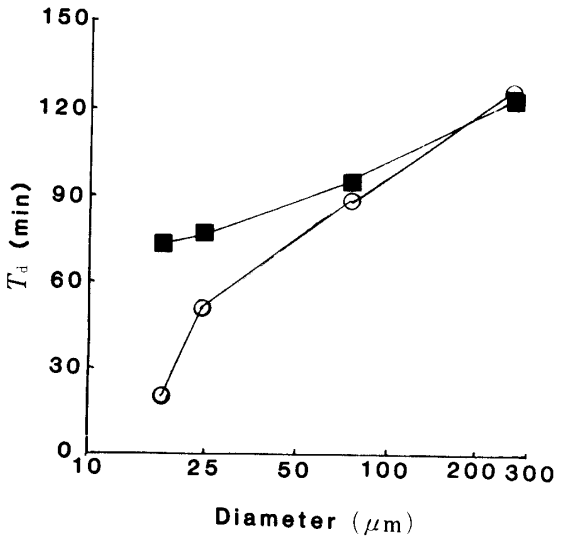

Fig. 11. Relationship between T_d and Particle Size in the Dissolution of FFA Powders

■, data for pH 6.24 phosphate buffer solution; ⊙, data for pH 6.24 phosphate buffer solution containing polysorbate 80 at the cmc.

solution containing polysorbate 80 at the cmc, are shown in Figs. 7 and 8, respectively, in which the full lines are regression curves of the Weibull distribution. The values of the probability parameters are shown in Table VI. The dissolution rate of the FFA powders was considerably enhanced as the particle size was reduced in the presence of polysorbate 80 at the cmc (Fig. 8), whereas it was not much increased in the absence of the surfactant (Fig. 7). The $S(t)$ values of FFA powders with various particle sizes are shown in Table VII and the resulting patterns are shown in Figs. 9 and 10. At the cmc of the surfactant, the initial values of $S(t)$ and the rate of decrease of $S(t)$ due to dissolution were enhanced as the particle size of FFA was micronized (Fig. 10), whereas no remarkable increase was observed in the absence of the surfactant (Fig. 9). T_d values of FFA powders of various particle sizes are plotted *vs.* logarithmic particle size in Fig. 11. It is evident that the enhancement of $S(t)$ by addition of polysorbate 80 is much greater with smaller particles. Thus, no remarkable increase of $S(t)$ generation rate ($1/T_d$) was observed on 42—48 mesh particles (263 μm), whereas the $S(t)$ generation rate of micronized powders obtained by crystallization (17.7 μm) was increased more than four-fold by addition of the surfactant. These results indicate that the wetting property of the powders is much improved for smaller particles, because they have large interfacial energy, resulting in an increase in their hydrophobicity.

Effect of Additives on the Available Surface Area of FFA

The surface characteristics of additives are also important factors in the dissolution behavior of solid dosage forms. The same analysis was therefore performed for FFA–additive 1 : 1 mixtures. The results of the dissolution tests on the FFA–additive mixtures in pH 6.24 phosphate buffer solutions are shown in Fig. 12. Furthermore, the probability parameters, the $S(t)$ values of FFA in the mixtures and the patterns obtained are shown in Tables VIII, IX and Fig. 13, respectively. The data in Table IX and Fig. 13 suggest that the enhancement of the dissolution rate for the FFA–PVP mixture is due to a significant increase of $S(t)$ generated by the hydrophilic properties of PVP, whereas that for the FFA–St.Mg mixture is lowered due to a decrease of $S(t)$ generated by the hydrophobic properties of St.Mg.

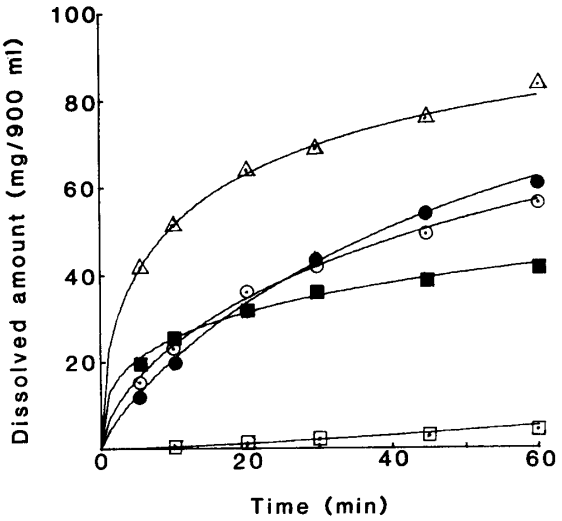

Fig. 12. Dissolution Profiles of FFA–Additive Mixtures in pH 6.24 Phosphate Buffer Solution ($W_0 = 100$ mg; $V = 900$ ml)

The full lines are the regression curves of the Weibull distribution.

△, FFA–PVP 1 : 1 mixture; ●, FFA–CS 1 : 1 mixture; ⊙, FFA–CMC-Ca 1 : 1 mixture; ■, FFA–MCC 1 : 1 mixture; ⊡, FFA–St.Mg 1 : 1 mixture.

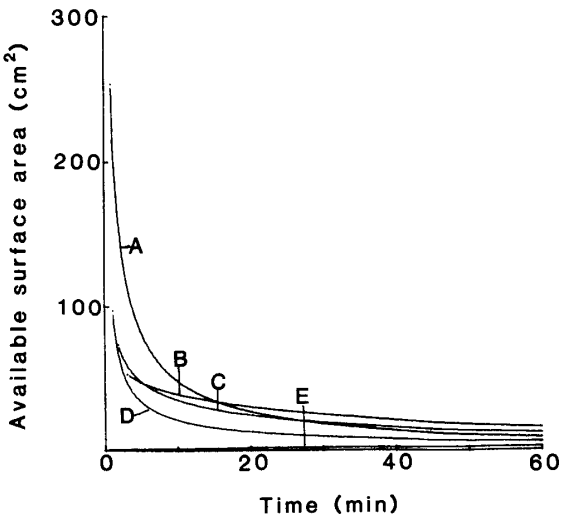

Fig. 13. $S(t)$ *vs.* t Patterns of FFA–Additive Mixtures in pH 6.24 Phosphate Buffer Solution

A, FFA–PVP 1 : 1 mixture; B, FFA–CS 1 : 1 mixture; C, FFA–CMC-Ca 1 : 1 mixture; D, FFA–MCC 1 : 1 mixture; E, FFA–St.Mg 1 : 1 mixture.

TABLE VIII. Probability Parameters of the Weibull Distribution in Fig. 12

Mixture (1 : 1)	a	b	T_{20} (min)	T_{50} (min)	T_d (min)
FFA–PVP	5.05	0.496	1.3	12.5	26.2
FFA–CS	35.1	0.833	11.8	46.1	71.6
FFA–CMC-Ca	19.5	0.651	9.6	54.6	95.9
FFA–MCC	9.32	0.364	7.5	168.2	460.5
FFA–St.Mg	5.88×10^3	1.36	196.2	451.4	591.0

TABLE IX. Available Surface Area of FFA–Additive Mixtures

Mixture (1 : 1)	Available surface area (cm^2/100 mg FFA) Time (min)									
	2	4	6	8	10	15	20	30	45	60
FFA–PVP	153.1	96.3	71.9	57.8	48.4	34.3	26.4	17.7	11.3	8.1
FFA–CS	58.7	50.3	45.3	41.7	38.9	33.6	29.8	24.2	18.6	14.8
FFA–CMC-Ca	70.7	53.0	44.3	38.7	34.7	28.1	23.9	18.6	14.0	11.2
FFA–MCC	64.0	40.0	29.7	24.2	20.6	15.3	12.3	9.1	6.6	5.2
FFA–St.Mg	0.9	1.1	1.3	1.4	1.5	1.8	2.0	2.3	2.6	2.8

In conclusion, a new method for evaluating the effect of wetting factors on dissolution behavior has been established. Thus, by using the probability parameters a, b, T_{20}, T_{50} and T_d, which could be obtained from linear regression of the dissolution data, the effects of varying the amounts of surfactant, particle size and additives on the time course of the available surface area of FFA during the dissolution process could be evaluated quantitatively.

References and Notes

1) This paper forms Part II of "Dissolution Profile in Relation to Available Surface Area." Parts of this work were presented at the 103rd Annual Meeting of the Pharmaceutical Society of Japan, Tokyo, 1983.
2) P. Finholt, H. Kristiansen, O. C. Schmidt and K. Wold, *Medd. Norsk. Farm. Selsk.*, **28**, 17 (1966).
3) N. Watari and N. Kaneniwa, *Chem. Pharm. Bull.*, **24**, 2577 (1976).
4) S. L. Lin, J. Menig and L. Lachman, *J. Pharm. Sci.*, **57**, 2143 (1968).
5) S. Kouchiwa, M. Nemoto, S. Itai, H. Murayama and T. Nagai, *Chem. Pharm. Bull.*, **33**, 1641 (1985).
6) A. W. Noyes and W. Whitney, *J. Am. Chem. Sci.*, **19**, 930 (1897).
7) J. G. Wagner, *J. Pharm. Sci.*, **58**, 1253 (1969).